

## 833. The Crystal Structure of the Mercury Dithizone Complex.

By MARJORIE M. HARDING (*née* AITKEN).

The mercury derivative of dithizone crystallises from aqueous pyridine as deep red solvated needles,  $\text{Hg}(\text{C}_{13}\text{H}_{11}\text{N}_4\text{S})_2 \cdot 2\text{C}_5\text{H}_5\text{N}$ . These have been studied by *X*-ray diffraction. They are orthorhombic, with  $a = 35.30$ ,  $b = 36.30$ ,  $c = 5.40$  Å, and space group *Fdd2*. The main features of the structure have been determined from Fourier projections down the *c*-axis and from a limited three-dimensional Fourier series. In the molecule of mercury dithizone, the mercury is bonded to one sulphur atom of each dithizone group; the Hg-S bond lengths are both 2.41 Å, and the S-Hg-S bond angle is 155°. A nitrogen atom from each azo-group is weakly co-ordinated to the mercury atom, making, with the sulphur atoms, a rather distorted tetrahedron around it. The dithizone groups are in an extended arrangement with no intramolecular hydrogen bonding.

ALTHOUGH dithizone,  $\text{NPh}\cdot\text{NH}\cdot\text{CS}\cdot\text{N}\cdot\text{NPh}$ , is a common reagent for the colorimetry of certain metals, the structure of the metal derivatives has remained uncertain. A crystal-structure determination by *X*-ray methods was therefore undertaken, and the mercury derivative,  $\text{Hg}(\text{C}_{13}\text{H}_{11}\text{N}_4\text{S})_2$ , was chosen because it could be obtained suitably crystalline. The deep red crystals contain pyridine of crystallisation which, as seen from their deterioration, they slowly lose on standing in air. They are orthorhombic, with cell dimensions  $a = 35.30 \pm 0.03$ ,  $b = 36.30 \pm 0.03$ ,  $c = 5.40 \pm 0.02$  Å. The needle axis is parallel to *c*; the space group is *Fdd2*. A density, 1.58 g. cm.<sup>-3</sup>, was found by flotation in aqueous potassium iodide solution, a procedure in which the loss of a little pyridine would be expected. The calculated density for eight molecules  $\text{Hg}(\text{C}_{13}\text{H}_{11}\text{N}_4\text{S})_2$  and sixteen molecules of pyridine per unit cell is 1.66 g. cm.<sup>-3</sup>; for eight unsolvated molecules it would be 1.35 g. cm.<sup>-3</sup>. The mercury atoms must lie in special positions on the two-fold axis. Further, the *z* parameter can be chosen arbitrarily as zero. The other atoms are in general positions, and the two dithizone residues of one molecule are related by a two-fold axis.

The *X*-ray photographs show a remarkably even fall in intensity of the *X*-ray reflections with increasing angle of reflection, because the scattering is predominantly by the mercury atoms at special positions in the lattice. Relatively small variations in this even fall are due to the contributions of the rest of the molecule; consequently the accuracy with which the co-ordinates of the light atoms could be found was limited.

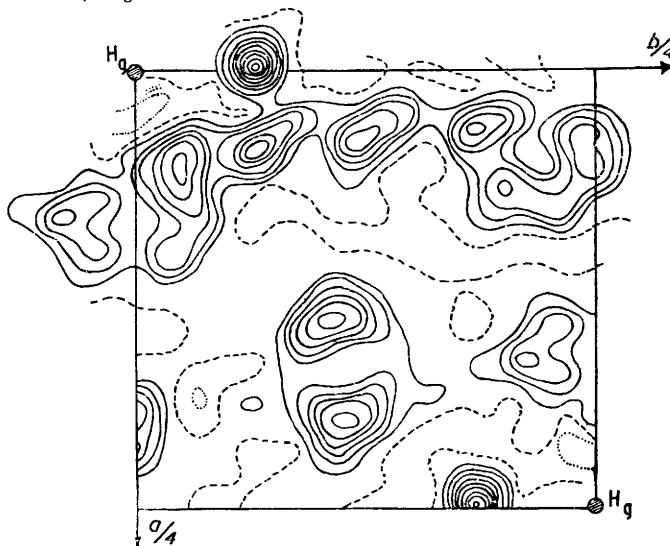
The intensities of the reflections in the layers with  $l = 0, 1, 2$ , and 3 were measured by visual estimation and converted to  $|\text{F}(hkl)|$  values.

## STRUCTURE DETERMINATION

(1) *The Electron-density Projection down the 001 Axis.*—A Patterson projection down the *c* axis confirmed the mercury positions. An electron-density projection was then calculated, using those terms whose signs are determined by the mercury atoms; it showed the sulphur atom clearly and one benzene ring. Some, and eventually all, of the remaining terms were then added, and the projection was further improved by "subtracting" the mercury atom to eliminate their diffraction effects. Thus the position of the remainder of the dithizone group was found, and also that of a molecule of pyridine of crystallisation. The final projection is shown in Fig. 1, and the atomic arrangement in Fig. 4. Table I gives the observed and calculated structure factors,  $\text{F}(hkl)$ . The agreement factor, *R* for all reflections (158) decreased from 27% for the mercury atom positions alone, to 12% in the present structure; the *R* factor for the 23 reflections to which mercury does not contribute, fell from over 50% in the first partial structure to 29% in the present structure.

(II) *Distribution of Atoms in Three Dimensions.*—The projection shows the extended arrangement of the dithizone group, the sulphur atom bonded to mercury, and a nitrogen atom fairly close to mercury. It cannot show whether the group S-Hg-S is linear; to do

FIG. 1. *Electron-density projection.*  $\rho(xy)$ , down the *c*-axis with the mercury atom at (0,0) subtracted. Contours at intervals of  $1 \text{ e \AA}^{-2}$  starting at  $2 \text{ e \AA}^{-2}$  (and at  $2 \text{ e \AA}^{-2}$  intervals on the sulphur atom); zero contour—broken line; negative contours—dotted lines.



this the atomic arrangement in the third dimension must be found. Here, calculation of the electron density in three dimensions was necessary, since projections down the *a* and *b* axes of the unit cell, both about  $35 \text{ \AA}$  long, could not show resolved atomic positions.

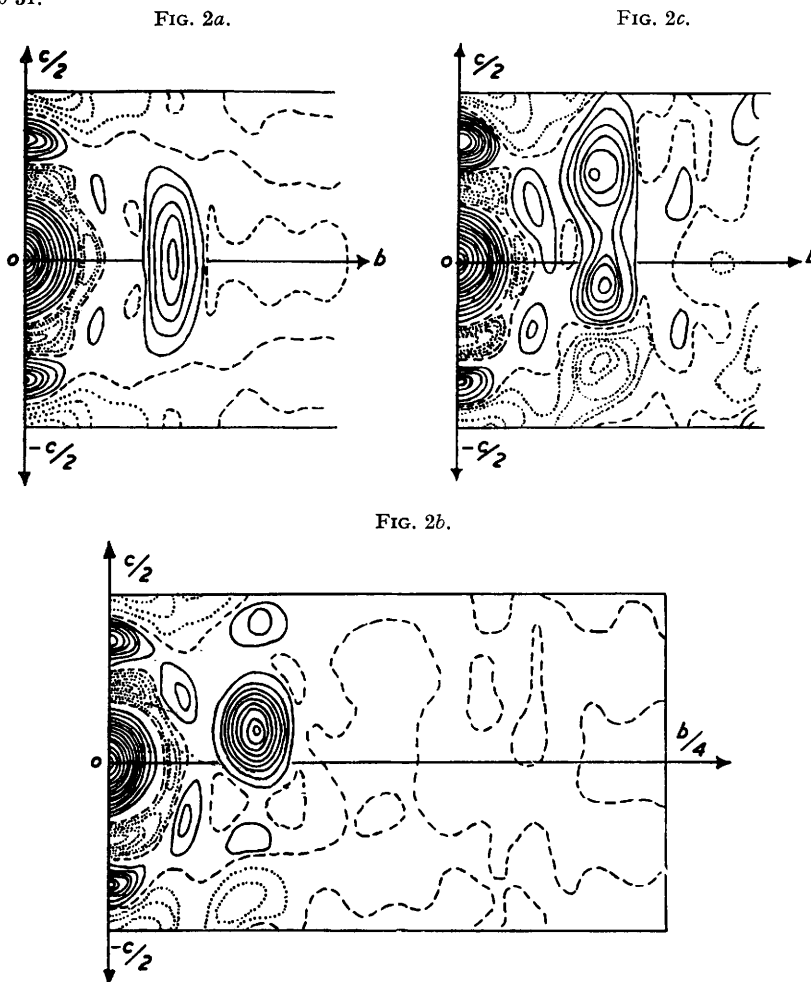
In three dimensions the structure is asymmetric, and the use of phase angles calculated

TABLE I. *Observed and calculated structure factors (one quarter of absolute values).*

F		F		F		F		F		F		F		F		F		F		
<i>h</i>	<i>k</i>	0 (obs.)	(calc.)	<i>h</i>	<i>k</i>	0 (obs.)	(calc.)	<i>h</i>	<i>k</i>	0 (obs.)	(calc.)	<i>h</i>	<i>k</i>	0 (obs.)	(calc.)	<i>h</i>	<i>k</i>	0 (obs.)	(calc.)	
4	0	0	182	219	30	6	0	54	61	18	14	0	117	125	14	22	0	48	55	
8	0	0	50	54	34	6	0	36	34	22	14	0	79	80	18	22	0	35	25	
12	0	0	92	84						26	14	0	64	77	22	22	0	58	41	
16	0	0	113	104	0	8	0	182	247	30	14	0	47	73	26	22	0	42	54	
20	0	0	125	130	4	8	0	72	79											
24	0	0	104	95	8	8	0	74	59	0	16	0	164	161	0	24	0	53	49	
28	0	0	97	121	12	8	0	60	22	4	16	0	185	201	4	24	0	62	76	
32	0	0	54	68	16	8	0	93	74	8	16	0	125	151	8	24	0	59	66	
					20	8	0	81	102	12	16	0	89	61	12	24	0	58	47	
2	2	0	180	202	24	8	0	57	54	16	16	0	124	96	16	24	0	42	33	
6	2	0	111	118	28	8	0	65	49	20	16	0	107	105	20	24	0	42	31	
10	2	0	202	206	32	8	0	37	27	24	16	0	82	92	24	24	0	37	38	
14	2	0	151	152						28	16	0	52	68						
18	2	0	129	136	2	10	0	70	81	32	16	0	48	60	2	26	0	71	68	
22	2	0	121	119	6	10	0	135	144						6	26	0	57	63	
26	2	0	89	88	10	10	0	108	99	2	18	0	63	60	10	26	0	59	55	
30	2	0	63	64	14	10	0	110	99	6	18	0	119	149	14	26	0	65	68	
34	2	0	42	47	18	10	0	80	65	10	18	0	124	122	18	26	0	37	29	
					22	10	0	55	48	14	18	0	124	125	22	26	0	54	49	
0	4	0	161	184	26	10	0	51	48	18	18	0	82	87						
4	4	0	120	112	30	10	0	60	59	22	18	0	86	90	0	28	0	74	60	
8	4	0	102	60						26	18	0	67	62	4	28	0	85	80	
12	4	0	177	178	0	12	0	93	60	30	18	0	36	44	8	28	0	75	66	
16	4	0	139	130	4	12	0	147	147						12	28	0	59	59	
20	4	0	99	94	8	12	0	141	143	0	20	0	68	43	16	28	0	64	62	
24	4	0	58	89	12	12	0	121	98	4	20	0	93	101	20	28	0	54	56	
28	4	0	71	66	16	12	0	114	103	8	20	0	94	95						
32	4	0	60	41	20	12	0	90	105	12	20	0	82	83	2	30	0	77	72	
					24	12	0	62	74	16	20	0	75	83	6	30	0	73	76	
2	6	0	123	119	28	12	0	83	65	20	20	0	57	61	10	30	0	74	86	
6	6	0	58	40	32	12	0	59	57	24	20	0	42	58	14	30	0	70	81	
10	6	0	137	144						28	20	0	37	43	18	30	0	64	60	
14	6	0	78	88	2	14	0	139	137						22	30	0	55	51	
18	6	0	101	103	6	14	0	183	174	2	22	0	41	28						
22	6	0	71	50	10	14	0	158	156	6	22	0	81	90	0	32	0	66	90	
26	6	0	62	47	14	14	0	108	110	10	22	0	67	78	4	32	0	63	78	

on the mercury-atom positions alone introduces false symmetry into the electron-density distributions. The extended distribution was calculated only after generalised projections and the section  $\rho(0yz)$  had been explored.

FIG. 2. Electron density in the section  $\rho(0yz)$  through the sulphur atom. Contours at intervals of  $10 \text{ e } \text{Å}^{-3}$  on the mercury atom and  $2 \text{ e } \text{Å}^{-3}$  elsewhere; zero contour—broken line; negative contours—dotted lines: (a) using phases for mercury only—or for mercury, and sulphur at  $z = 0$ ; (b) using phases for mercury, and for sulphur at  $z = 0.10$ ; (c) using phases for mercury, and for sulphur at  $z = 0.31$ .



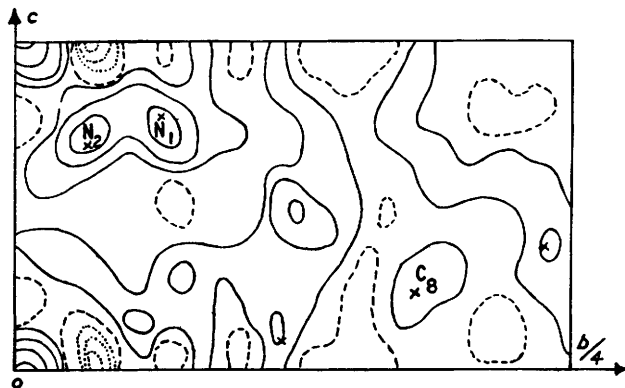
(a) *Generalised projections.* Since the  $c$  axis is short,  $5.4 \text{ Å}$ , it seemed likely that the  $z$  parameters of the atoms could be determined from two generalised projections calculated with the  $(hk1)$  and  $(hk2)$   $F$  values and mercury-atom phases. In both these projections peaks occur at the expected sulphur-atom sites, but the rest of the pattern is very confused. The heights of the sulphur-atom peaks suggested that the sulphur atom is not at  $z = 0$  but has a  $z$  co-ordinate  $0.10$ — $0.15$ .

(b) *Section  $\rho(0yz)$ .* The first-section  $\rho(0yz)$  calculated with mercury phase angles confirmed the impression that the sulphur is not at  $z = 0$ . It showed a much elongated peak (Fig. 2a) from which a parameter of  $z \sim 0.1$  could be inferred. This deduction was checked by calculating two additional electron-density distributions:  $\rho(0yz)$  in Fig. 2b

has phase angles calculated for mercury at  $z = 0$  and sulphur at  $z = 0.10$ ;  $\rho(0yz)$  in Fig. 2c has phase angles calculated for mercury at  $z = 0$  and sulphur at  $z = 0.31$ . Fig. 2b shows a single peak at  $z = 0.1$ . Fig. 2c shows peaks both at the position used in the phase angle calculation and at  $\pm z = 0.1$ .

The appearance of Fig. 2a and 2c has a close parallel in the effects of wrong phasing observed in other asymmetric syntheses, e.g., in the hexacarboxylic acid of vitamin B<sub>12</sub>.<sup>1</sup> Peaks about two-thirds of the expected height appear at wrongly assumed positions, and smaller peaks at the correct atom positions. The positions assumed here in Fig. 2a and 2c correspond to linear and tetrahedral S-Hg-S angles. It is clear that neither assumption is as satisfactory as that used in Fig. 2b where a single peak appears at  $z = 0.1$ . This leads to an angle S-Hg-S of 155°.

FIG. 3. Section,  $\rho(5/120, y, 0)$ , of the electron density. Contours at intervals of  $1 \text{ e } \text{Å}^{-3}$ ; zero contour, broken line; negative contours, dotted lines.



(c) *Three-dimensional electron-density series.* This was finally calculated, phased by mercury and sulphur in the position found above. It was expected that the phase angles would be sufficiently accurate to show the light-atom peaks clearly. But the electron-density maps are very confused; peaks range from 1 to  $4\frac{1}{2} \text{ e } \text{Å}^{-3}$  in height and are distorted or spread over large areas. By using the projection, and known bond lengths, it was possible to place most of the atoms in regions of  $2 \text{ e } \text{Å}^{-3}$  or more, near or on peaks, but a few atoms are in regions of only 1 or  $1\frac{1}{2} \text{ e } \text{Å}^{-3}$ . There are also many spurious peaks not corresponding to atomic positions. A typical section is shown in Fig. 3.

Approximate  $z$  co-ordinates had previously been found by arranging a model over the (001) Fourier projection, and were compared with those of the three-dimensional series. The tilt of the benzene ring C<sub>2</sub>-C<sub>7</sub> was appreciably altered, and that of the ring C<sub>8</sub>-C<sub>13</sub> was slightly altered, with corresponding small changes in the -N-N- chain.

Diffraction effects around the mercury atom are serious, and the incompleteness of the data limits the possible accuracy of the series. But the incompleteness of the phasing and the false symmetry also contribute to the confusion in the electron-density maps. The importance of a heavy atom in determining the scattered intensities depends on the ratio  $f_{\text{heavy atom}}^2 / \sum f_{\text{all atoms}}^2$  (equal to 0.735 here), and so should its effectiveness in phasing a Fourier series. According to Luzzatti,<sup>2</sup> who gives the light-atom peaks to be expected in a three-dimensional Fourier series as a function of this ratio, the carbon and nitrogen peaks in mercury dithizone should be 3.5 and 4.1  $\text{e } \text{Å}^{-3}$  respectively; many of them are found in the range 3-4  $\text{e } \text{Å}^{-3}$ . The difficulty in interpretation arises not because the peaks are too low, but because of the many distortions and spurious peaks.

The partial false symmetry is introduced by using phase angles based on atoms in or

<sup>1</sup> Pickworth, D.Phil. Thesis, Oxford, 1955, p. 68.

<sup>2</sup> Luzzatti, *Acta Cryst.*, 1953, **6**, 142.

near special positions. If all the phases used were derived from the positions Hg at  $0,0,0$ ; S at  $0,y,0$ , there would be centres of symmetry at  $\frac{1}{8}, \frac{1}{8}, \frac{1}{8}$ , and  $\frac{1}{8}, \frac{1}{8}, \frac{5}{8}$ , etc. The phases used for  $F(hk1)$ ,  $F(hk2)$ , and  $F(hk3)$  are derived from Hg at  $0,0,0$ ; S at  $0,y,0.1$ , and so are

FIG. 4. *The atomic arrangement in projection down the c-axis.*

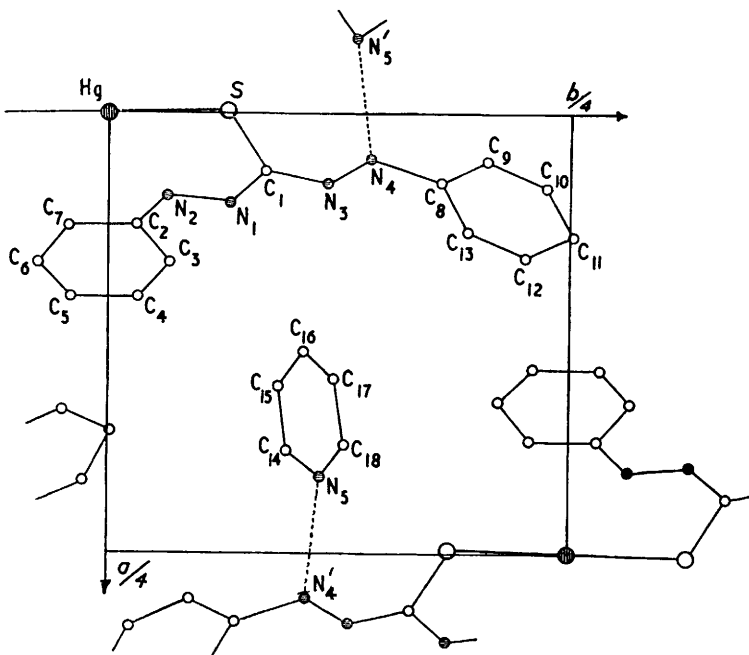
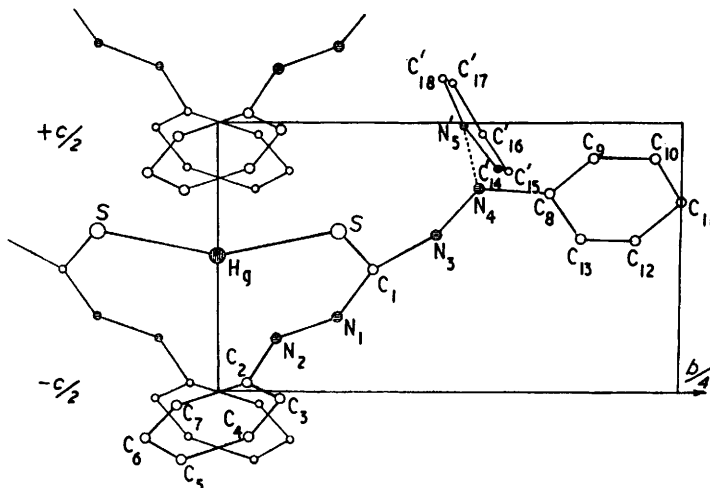


FIG. 5. *The atomic arrangement in projection down the a-axis.*



nearly centrosymmetric. But the *signs* used for  $F(hk0)$ , with no mercury contributions, are derived from the known atomic positions in projection and do not give these centres of symmetry. The extra symmetry is obvious when appropriate Fourier sections are compared; for instance, the large spurious peak in the section in Fig. 3 is related to  $N_5$  in the pyridine molecule.

Further work on the three-dimensional data is not being carried out at present, but may be considered later when more computing facilities are available. No doubt the appearance of the three-dimensional electron-density series could be greatly improved by using phase angles, including the light-atom positions, but even then, no great accuracy in interatomic distances would be expected.

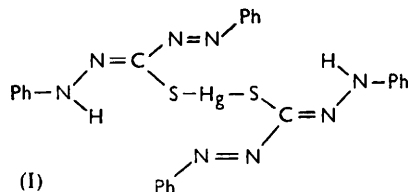
#### DESCRIPTION OF THE STRUCTURE AND DISCUSSION.

The atomic arrangement is shown in Figs. 4 and 5, and the atomic co-ordinates are given in Table 2. The co-ordinates of the sulphur atom are probably accurate to  $\pm 0.04 \text{ \AA}$ ; those of carbon and nitrogen atoms are much more approximate.

TABLE 2. *Fractional atomic co-ordinates.*

Hg	$x$	$y$	$z$		$x$	$y$	$z$		$x$	$y$	$z$
	0	0	0								
S	0.247	0.185	0.345	C <sub>8</sub>	0.038	0.180	0.24	N <sub>1</sub>	0.050	0.066	0.78
				C <sub>9</sub>	0.026	0.203	0.37	N <sub>2</sub>	0.045	0.033	0.70
C <sub>1</sub>	0.033	0.084	0.95	C <sub>10</sub>	0.042	0.237	0.36	N <sub>3</sub>	0.040	0.118	0.085
C <sub>2</sub>	0.064	0.016	0.525	C <sub>11</sub>	0.183	0.001	0.97	N <sub>4</sub>	0.025	0.124	0.25
C <sub>3</sub>	0.087	0.034	0.475	C <sub>12</sub>	0.082	0.227	0.06				
C <sub>4</sub>	0.103	0.017	0.32	C <sub>13</sub>	0.067	0.196	0.07	C <sub>14</sub>	0.192	0.098	0.595
C <sub>5</sub>	0.147	0.230	0.50					C <sub>15</sub>	0.163	0.092	0.575
C <sub>6</sub>	0.166	0.212	0.565					C <sub>16</sub>	0.134	0.105	0.71
C <sub>7</sub>	0.187	0.228	0.70					C <sub>17</sub>	0.150	0.123	0.90
								C <sub>18</sub>	0.188	0.128	0.92
								N <sub>5</sub>	0.207	0.116	0.75

The primary bonding of dithizone to mercury is through the sulphur atom, but a nitrogen atom of the azo-group is also weakly co-ordinated to the mercury. The dithizone group is in an extended form, with no possibility of internal hydrogen bonding. The molecule can be written as in (I). There is probably a hydrogen bond between the NH group (N<sub>4</sub>) and the pyridine nitrogen (N<sub>5</sub>); the distance N<sub>4</sub>-N<sub>5</sub> is less than 3 Å, but the atoms C<sub>16</sub> . . . . N<sub>5</sub> . . . . N<sub>4</sub> depart considerably from a straight line.



The packing arrangement is shown in Fig. 6. The space which the pyridine molecules occupy is like a channel parallel to the  $c$ -axis; this should account for the easy loss of pyridine from the crystals in air. The highest measured density corresponds to 75% of the theoretical pyridine content in  $\text{Hg}(\text{C}_{13}\text{H}_{11}\text{N}_4\text{S})_2 \cdot 2\text{C}_5\text{H}_5\text{N}$ , but some pyridine would almost certainly be lost in the density measurement in an aqueous solution.

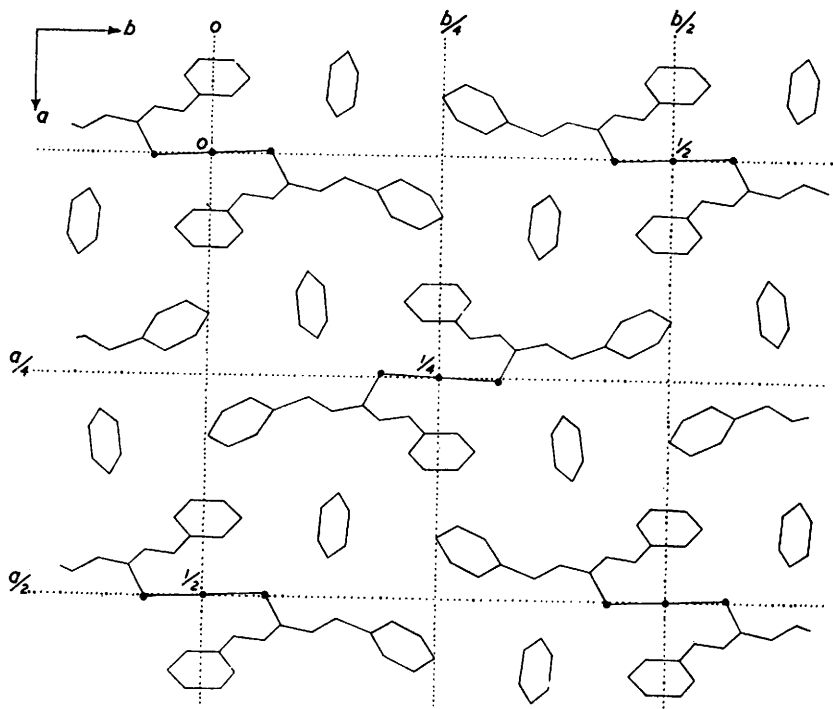
Probably all metal dithizonates are similarly bonded through sulphur with nitrogen co-ordination; a more nearly tetrahedral arrangement around the metal atom would seem likely with other metals, especially those with smaller atomic radius. Crystalline zinc dithizone has been obtained but is not isomorphous with mercury dithizone. [It is possible, of course, that in the dithizonates of cobalt, nickel, zinc, etc., metal-nitrogen bonding might be favoured, just as in the series of complex thiocyanates,  $\text{K}_2\text{M}(\text{SCN})_4$ , when M is Zn, Cr, or Co there is metal-nitrogen bonding, but when M is Rh, Ag, Cd, or Pt, there is metal-sulphur bonding.<sup>3</sup>]

A most interesting feature of the structure is the co-ordination group around mercury,

<sup>3</sup> Zhdanov and Zvonkova, 13th Conference, I.U.P.A.C., 1953 (Stockholm), p. 153.

shown in Fig. 7. The Hg-S bond length,  $2.4_1 \text{ \AA}$ , is normal for a covalent bond, but the Hg-N distance,  $2.5\text{--}2.6 \text{ \AA}$ , and the angle, S-Hg-S, of  $155^\circ$  are quite unusual. Even

FIG. 6. Projection down the *c*-axis showing the packing of molecules. (The *z*-co-ordinates of the mercury atoms are shown.)



after allowance for a possible error of  $0.2 \text{ \AA}$  in the Hg-N distance, it is significantly different from either a covalent bond ( $\sim 2.1 \text{ \AA}$ ) or a van der Waals contact. The arrangement is best described as a distortion of linear (*sp*) bicovalent mercury, S-Hg-S, due to the approach of the two nitrogen atoms and the formation of weak, secondary, Hg...N bonds. A similar arrangement has been reported in one other compound,  $\text{KHg}(\text{SCN})_3$ .<sup>4</sup> Here mercury is bonded to two sulphur atoms at  $2.4 \text{ \AA}$ , making an angle at mercury of

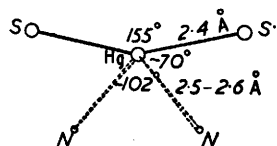


FIG. 7. The co-ordination group around the mercury atom.

approximately  $155^\circ$ ; two more sulphur atoms, at about  $2.8 \text{ \AA}$ , complete a very distorted tetrahedron.

A survey of mercury compounds (other than regular tetrahedral ones) shows that small deviations from linearity frequently occur. Also, many mercury derivatives, such as diphenylmercury, have appreciable dipole moments in benzene and other organic solvents, corresponding to bond angles in the region of  $150^\circ$ —presumably with some solvation.<sup>5</sup> All this evidence suggests that deviation from linearity does not greatly affect the energy of  $-\text{X}-\text{Hg}-\text{X}-$ ; therefore when, by such deviation, additional weak bond formation becomes possible, the energy change is favourable.

<sup>4</sup> Zhdanov and Sanadse, *Zhur. Fiz. Khim.*, 1952, **26**, 469.

<sup>5</sup> Kadomtzeff, *Compt. rend.*, 1949, **228**, 681.

## EXPERIMENTAL

*Preparation of Crystals.*—Mercury dithizone was prepared as described by Irving *et al.*<sup>6</sup> and deep red needles were obtained by crystallisation from aqueous pyridine. They deteriorated slowly in air, probably by loss of solvent. They were not analysed, because the analysis of crystals, dried (and therefore containing no pyridine), was reported by Irving *et al.* and was satisfactory.

*Preliminary Data.*—Oscillation photographs and Weissenberg photographs about the needle axis were taken. The cell dimensions were determined from Weissenberg photographs, calibrated with copper powder lines. Only the reflections  $hkl$ , with  $h + k = 2n$ ,  $k + l = 2n$ ;  $0kl$ , with  $k = 4n$ ; and  $h0l$ , with  $h = 4n$ , were observed, so the space group is  $Fdd2$ . In this space group there are 16 general equivalent positions. The eight mercury atoms must be in the special positions on the two-fold axes. It was observed that, in addition to the above space-group absences, nearly all the reflections  $hk0$ ,  $hk2$ , with  $h + k + l = 4n + 2$ , are either weak or absent, showing again that the mercury atoms lie on the two-fold axes. The  $z$  parameter of one can be arbitrarily chosen as zero, so the mercury positions are  $0,0,0$ ;  $\frac{1}{4}, \frac{1}{4}, \frac{1}{4}$ ; etc.

The density data are given on p. 4136.

*Intensity Measurements.*—Weissenberg photographs on multiple films were taken, with  $Cu-K\alpha$  radiation, for the layers  $hk0$ ,  $hk1$ ,  $hk2$ , and  $hk3$ . Because of deterioration of the crystals a fresh one was required for each layer. The intensities were measured visually, and Lorentz and polarisation corrections applied. Reflections with  $\sin \theta/\lambda \geq 0.5$  were observed on some photographs but were rather weak for satisfactory measurement.

*Absorption Corrections.*—The linear absorption coefficient is  $112 \text{ cm}^{-1}$ . The rotation axis of the crystals in all the Weissenberg photographs was parallel to the needle axis,  $c$ , and the cross-section was roughly square with sides about  $0.04 \text{ mm}$ . Absorption corrections were estimated for 70 of the  $hk0$  reflections by a graphical method, based on that of Albrecht.<sup>7</sup> It was found that, provided the cross-section of each crystal used was approximately square, and the sides less than *ca.*  $1 \text{ mm}$ ., no correction need be made.

*Scale and Temperature Factors.*—The temperature factor was determined by Wilson's method,<sup>8</sup> and  $B = 2.7_6 \text{ \AA}^2$  was found. The atomic scattering factors used were: for carbon and nitrogen, those of Macgillavry;<sup>9</sup> for hydrogen, that of McWeeney;<sup>10</sup> and for mercury, that of James and Brindley.<sup>11</sup> (The work was done before Thomas and Umeda's mercury scattering factor<sup>12</sup> was published.) The absolute scale factor cannot be determined by Wilson's method here, on account of the mercury atoms in special positions; it was determined by a comparison of observed and calculated structure factors. Later the scale and temperature factors were checked by plotting  $\log \langle F_{\text{obs.}}(hk0)/|F_{\text{calc.}}(hk0)| \rangle_s$  against  $\sin^2 \theta/\lambda^2$ , (where  $\langle \rangle_s$  signifies an average over a range of  $\sin^2 \theta$  values); no change in  $B$  greater than  $0.1 \text{ \AA}^2$  was indicated.

*Calculation of the Fourier Projections and Sections, and of Structure Factors.*—All these summations were done by punched card methods on Hollerith machines. In the  $[001]$  projection, which is centrosymmetric, there were 135 terms whose signs were determined by mercury, and 23 to which the mercury does not contribute. In the refinement the series  $(F_{\text{obs.}} - F_{\text{Hg}})$  was used.

In the generalised projections the components  $C_L(xy)$  and  $S_L(xy)$  of  $\rho_L(xy)$  were calculated, mercury phases being used.

Phase angles for the three-dimensional series were calculated by hand; the assumption can be made that  $x_s = 0$  (or  $0.25$ ), which makes the phase angle independent of  $h$ .

The three-dimensional Fourier series was calculated on "Deuce" at the National Physical Laboratory, the phases calculated for the sections above being used. Because these are independent of  $h$ , it was possible to use a simplified form of the electron-density expression.

I thank Mrs. D. M. Hodgkin for help and encouragement; also Dr. H. M. N. Irving for suggesting the problem, and Dr. J. S. Rollett for the Fourier calculation on "Deuce."

CHEMICAL CRYSTALLOGRAPHY LABORATORY,  
SOUTH PARKS ROAD, OXFORD.

[Received, June 2nd, 1958.]

<sup>6</sup> Irving, Andrew, and Risdon, *J.*, 1949, 541.

<sup>7</sup> Albrecht, *Rev. Sci. Instr.*, 1939, **10**, 221.

<sup>8</sup> Wilson, *Nature*, 1942, **150**, 152.

<sup>9</sup> Macgillavry, *Acta Cryst.*, 1955, **8**, 478.

<sup>10</sup> McWeeney, *ibid.*, 1951, **4**, 513.

<sup>11</sup> Internationale Tabellen zur Bestimmung von Kristallstrukturen, Berlin, 1935.

<sup>12</sup> Thomas and Umeda, *J. Chem. Phys.*, 1957, **26**, 293.